

Orbital polarons and ferromagnetic insulators in manganites

T. Mizokawa

Department of Complexity Science and Engineering, Graduate School of Frontier Science, University of Tokyo, Bunkyo-ku, Tokyo 113-0033, Japan

D. I. Khomskii and G. A. Sawatzky

Solid State Physics Laboratory, Materials Science Centre, University of Groningen, Nijenborgh 4, 9747 AG Groningen, The Netherlands

(November 1, 2018)

We argue that in lightly hole doped perovskite-type Mn oxides the holes (Mn^{4+} sites) are surrounded by nearest neighbor Mn^{3+} sites in which the occupied $3d$ orbitals have their lobes directed towards the central hole (Mn^{4+}) site and with spins coupled ferromagnetically to the central spin. This composite object, which can be viewed as a combined orbital-spin-lattice polaron, is accompanied by the breathing type (Mn^{4+}) and Jahn-Teller type (Mn^{3+}) local lattice distortions. We present calculations which indicate that for certain doping levels these orbital polarons may crystallize into a charge and orbitally ordered ferromagnetic insulating state.

I. INTRODUCTION

The interplay between the magnetic and electric properties of $R_{1-x}A_x\text{MnO}_3$ (R is a trivalent rare-earth ion and A is a divalent alkaline-earth ion) has been extensively studied in the light of basic physics as well as their technological importance.^{1,2} La/Sr and La/Ca based compounds $\text{La}_{1-x}\text{Sr}_x\text{MnO}_3$ and $\text{La}_{1-x}\text{Ca}_x\text{MnO}_3$ are metallic below the Curie temperature for $0.15 < x < 0.5$. While the transport properties of the La/Sr system with $x = 0.3$ are well described by the conventional double exchange theory,^{2,3} the La/Ca system ($x \sim 0.3$) shows the colossal magnetoresistance (CMR) behavior which cannot be explained by the double exchange mechanism.⁴ Neutron diffraction and x-ray absorption measurements of the La/Ca system indicate that the small magnetic polarons, in which spins are ferromagnetically aligned, play a role in the CMR effect.^{5,6} Recently, it was suggested that phase separation between the ferromagnetic metal (FM) region and the antiferromagnetic insulator (AFI) region is essential for the CMR behavior⁷ and, actually, the coexistence of the FM and AFI clusters has been observed in La/Ca.⁸ On the other hand, $\text{Pr}_{1-x}\text{Ca}_x\text{MnO}_3$ is insulating for all x ; it has the AFI phase for $0.3 < x < 0.5$ and the ferromagnetic insulator (FI) phase for $0.1 < x < 0.3$ ^{9,10} although the structural details are still not elucidated.¹¹ It has been reported that in the Pr/Ca system, while the magnetic moments are almost ferromagnetically aligned for $x \sim 0.2$, they are canted for $x \sim 0.1$ and 0.3 , namely, near the boundary between the AFI and FI phases.^{9,10} Recently, it has been found that the La/Sr system of $0.10 < x < 0.15$ exhibits a FI behavior at low temperature and may have charge and orbital ordering.^{12,13} This all raises a question as to the origin of the FI phase in the Pr/Ca system with $x \sim 0.2$ while the La/Sr system with similar hole concentrations are ferromagnetic metals.

In this work, we study a charge and orbitally ordered

state which can be viewed as an orbital polaron lattice and which produces the fully polarized FI state for $x = 1/4$. Hartree-Fock (HF) calculations on d - p -type lattice models show that the magnetic coupling between the orbital polarons is actually ferromagnetic and support this idea. We also shortly discuss the evolution from the FI state at $x = 1/4$ to the AFI state at $x = 1/2$ in $\text{Pr}_{1-x}\text{Ca}_x\text{MnO}_3$ as well as the relationship between the orbital polarons and the small ferromagnetic polarons observed in $\text{La}_{1-x}\text{Ca}_x\text{MnO}_3$.

II. ORBITAL POLARON

First, let us explain the basic idea underlying the concept of orbital polarons (see also ref.¹⁴). Since the electronic configuration of Mn^{3+} in $R\text{MnO}_3$ is $t_{2g}^3e_g^1$, in an octahedral coordination, there exists double orbital degeneracy and a strong Jahn-Teller effect. On the other hand, the e_g orbitals are empty in Mn^{4+} . When one dopes $R\text{MnO}_3$ with holes, namely, puts Mn^{4+} ions in the background of the Mn^{3+} ions, the e_g orbitals of all the Mn^{3+} site surrounding the Mn^{4+} site tend to be directed towards it as displayed in Fig. 1. Such an orbital orientation occurs for two reasons. One is simply steric: oxygen ions sitting in between the Mn ions move towards the Mn^{4+} site and, consequently, the MnO_6 octahedra of the neighboring Mn^{3+} sites are elongated along the axis pointing to the Mn^{4+} site. Another factor is that the orbital occupation helps to optimize the covalency between the Mn^{3+} and Mn^{4+} sites: the e_g orbitals directed towards Mn^{4+} site allow for maximal Mn-O-Mn hopping. An important consequence of such an orbital ordering is that, according to the Goodenough-Kanamori rules, the exchange interaction between the Mn^{3+} and Mn^{4+} in this cluster is ferromagnetic. Thus one can treat this object simultaneously as a lattice (both breathing-type and Jahn-Teller-type) polaron, a ferromagnetic polaron,

and an orbital polaron.

For $x = 1/4$, one can expect a very natural type of ordering of these polarons shown in Fig. 2. In this polaron lattice, the orbital polarons form a body-centered cubic lattice which have two such polarons per unit cell. Therefore, one can divide the orbital polaron lattice into two sublattices which are simple cubic lattices labeled as A and B . In Fig. 2, the shaded (open) circles and orbitals indicate the Mn^{4+} and Mn^{3+} sites in sublattice A (B). In each sublattice, since the neighboring orbital polarons share the Mn^{3+} sites, the coupling between them is very strong and ferromagnetic. On the other hand, it is not trivial whether the coupling between the neighboring orbital polarons belonging to the different sublattices is ferromagnetic or antiferromagnetic. In order to see whether the magnetic coupling between sublattices A and B is ferromagnetic or not and to check the stability of this ordered structure (which is actually a form of charge ordering (CO)), we performed HF calculation on the perovskite-type lattice model with the Mn $3d$ and O $2p$ orbitals under the lattice distortion shown in Fig. 1.

III. MODEL HARTREE-FOCK CALCULATION

We employ the multi-band d - p model with 16 Mn and 48 oxygen sites in which full degeneracy of Mn $3d$ orbitals and the O $2p$ orbitals are taken into account. In this model, the intra-atomic Coulomb interaction between the $3d$ electrons is considered in terms of Kanamori parameters u , u' , j and j' . The charge-transfer energy Δ is defined by $\epsilon_d^0 - \epsilon_p + nU$, where ϵ_d^0 and ϵ_p are the energies of the bare $3d$ and $2p$ orbitals and $U (= u - 20/9j)$ is the multiplet-averaged d - d Coulomb interaction. The transfer integrals between Mn $3d$ and O $2p$ orbitals are given in terms of Slater-Koster parameters ($pd\sigma$) and ($pd\pi$) and those between the O $2p$ orbitals are expressed by ($pp\sigma$) and ($pp\pi$). Here, the ratio ($pd\sigma$)/($pd\pi$) is -2.16. Δ , U , and ($pd\sigma$) for RMnO_3 are 4.0, 5.5, and -1.8 eV, respectively, which are deduced from the photoemission studies¹⁶ and *ab-initio* band-structure calculations.^{17,18} ($pp\sigma$) and ($pp\pi$) are fixed at -0.60 and 0.15 for the undistorted lattice, which are close to the values widely used for various $3d$ transition-metal oxides.¹⁷

The t_{2g} - t_{2g} antiferromagnetic coupling is correctly captured by the present method which can reproduce the A -type AFI state for LaMnO_3 and the G -type AFI state for LaCrO_3 .¹⁹ When the lattice is distorted, the transfer integrals are scaled using Harrison's prescription. In this model calculation, Δ is the most important parameter and the other parameters are not sensitive to the calculated result. Since Δ typically has an error bar of ± 1 eV, we have performed calculations for $\Delta = 2.0$ and 6.0 eV and confirmed that our conclusion is not changed. In this work, the magnitude of the distortion is given by the ratio $(d_l - d_s)/d$ where d_s is the Mn-O bond length at the Mn^{4+} site and d_l is the longest Mn-O bond at the Mn^{3+} site.

$d = (d_l + d_s)/2$ is the Mn-O bond length before the lattice distortion is included. Please note that ($dd\sigma$), ($dd\pi$), and ($ddd\delta$) between the Mn $3d$ orbitals have been neglected. This is because, in the perovskite structure, the shortest distance between the Mn ions is approximately $2d$ (~ 4 Å) and that, using the Harrison's relation,¹⁷ ($dd\sigma$), ($dd\pi$), and ($ddd\delta$) are ~ -0.08 , 0.04, and -0.01 eV which are very small compared to ($pd\sigma$) and ($pd\pi$). Therefore, the effective d band width mainly arises from ($pd\sigma$) and ($pd\pi$) in the perovskites.

In Fig. 3, the energy difference between the ferromagnetic state and the AFI state, where the two sublattices are antiferromagnetically coupled, is plotted for $x = 1/4$ as a function of the distortion of the oxygen octahedron $(d_l - d_s)/d$. The postulated distortion compatible with the orbital polaron is justified by the fact that the AFI state with the orbital polaron exists as a meta-stable solution even without the lattice distortion. Without the lattice distortion, the FM state is lower in energy than the AFI state. The distortion larger than 0.075 opens a band gap for the ferromagnetic state and induces the FM to FI transition. As plotted in Fig. 3, the magnitude of the band gap increases monotonically with the lattice distortion exceeding the critical one ~ 0.065 . The magnitude of the charge ordering, namely, the difference of the occupation between the Mn^{3+} and Mn^{4+} sites (ΔN_d) also increases with the lattice distortion ($\Delta N_d \sim 0.7$ for $(d_l - d_s)/d = 0.1$).

The FI state found here is exactly the orbital polaron lattice shown in Fig. 2. Interestingly, under the lattice distortion, the FI state is still lower in energy than the AFI state. This indicates that the magnetic coupling between two orbital polarons in different sublattices is also ferromagnetic. In the FI state, the oxygen between the two Mn^{3+} sites has hole concentration of ~ 0.2 which is as large as that in the oxygen between the Mn^{3+} and Mn^{4+} sites. Namely, the holes at the Mn^{4+} site are partially transferred to the oxygen between the two Mn^{3+} sites and make the Mn^{3+} - Mn^{3+} coupling ferromagnetic. Therefore, the Mn^{3+} - Mn^{3+} coupling at $x = 1/4$ is different from that at $x = 0$. In this case, once the band gap opens due to the lattice distortion, the energy difference between the FI and AFI states is not sensitive to the magnitude of the distortion. Here, it should be noted that the FM state without lattice distortion is homogeneous and metallic, indicating that the lattice distortion is essential to stabilize the orbital polarons and realize the CO FI state. The orbital polaron lattice, namely, the FI state with the polaron-type charge and orbital ordering might be responsible for the FI phase found in $\text{Pr}_{1-x}\text{Ca}_x\text{MnO}_3$ for $0.1 < x < 0.3$.⁹⁻¹¹ In the La/Sr system, the lattice distortion is suppressed and the orbital polaron is not formed. On the other hand, in the Pr/Ca system, the lattice distortion is favored and the orbital polaron lattice would be stabilized.

IV. COMPARISON BETWEEN CHARGE ORDERINGS AT $x = 1/8, 1/4$ AND $1/2$

The charge and orbital ordering in the xy -plane of the orbital polaron lattice is shown in Fig. 4(a) for $x = 1/4$. One can visualize it as the orbital zigzags constructed from the $3x^2 - r^2/3y^2 - r^2$ orbitals and the Mn^{4+} sites which are arranged in a staggered way, so that the neighboring zigzags (shown by the thick solid and broken lines) meet at the Mn^{4+} sites. In the CE -type AFI state for $0.3 < x < 0.5$,⁹ the non-crossing zigzag is stabilized by the Jahn-Teller distortion at the Mn^{3+} site²⁰ and the charge and orbital ordering along the zigzags²¹ is shown in Fig. 4(b). Thus this orbital ordering is quite different from the one suggested above for $x = 1/4$. It would be interesting to see how the orbital polaron lattice for $x = 1/4$ evolves to the CE -type AFI state with charge and orbital ordering for $x = 1/2$ which consists of non-crossing orbital zigzag: via continuous flipping of "broken" zigzags of Fig. 4(a) or as a first order phase transition with eventual phase separation into "1/4"-like and "1/2"-like phases.

It is instructive to describe the difference between two FI states which the model HF calculations give for $\text{Pr}_{3/4}\text{Ca}_{1/4}\text{MnO}_3$ (this work) and for $\text{La}_{7/8}\text{Sr}_{1/8}\text{MnO}_3$.¹⁵ The calculations for $x = 1/8$ show that some ferromagnetic states with orbital and charge modulations are stable even without a lattice distortion. The predicted FI state with charge and orbital ordering for $\text{La}_{7/8}\text{Sr}_{1/8}\text{MnO}_3$ has the hole-rich and hole-poor planes alternating along the z -axis. Since the orbital ordering in the hole-poor plane is essentially the same as that in LaMnO_3 , a small amount of lattice distortion can open a band gap.¹⁵ The calculated results qualitatively agree with the experimental facts that $\text{La}_{1-x}\text{Sr}_x\text{MnO}_3$ of $x = 1/8$ is a FI state with orbital ordering but does not have substantial lattice distortion.^{12,13} On the other hand, at $x = 1/4$, the homogeneous FM state is very stable and no FI state with orbital and charge modulations is obtained unless a large lattice distortion is included. In the FI state obtained for $\text{Pr}_{3/4}\text{Ca}_{1/4}\text{MnO}_3$, the large lattice distortions of the Jahn-Teller and breathing type are required to open a band gap. $\text{Pr}_{3/4}\text{Ca}_{1/4}\text{MnO}_3$ can be insulating probably because the large buckling of the Mn-O-Mn bonds ($\angle \text{Mn-O-Mn} \sim 155^\circ$)⁹ reduces the band width of the e_g band and allows the oxygen ions to relax easily. In this sense, the FI state in $\text{La}_{7/8}\text{Sr}_{1/8}\text{MnO}_3$ is in the weak coupling limit and is different from the FI state for $\text{Pr}_{3/4}\text{Ca}_{1/4}\text{MnO}_3$ which requires the strong electron-lattice coupling. $\text{La}_{3/4}\text{Sr}_{1/4}\text{MnO}_3$ however remains a ferromagnetic metal because the straight Mn-O-Mn bonds make the bandwidth relatively large and increase the frequency of the Mn-O stretching mode.

It is expected that the electron-lattice coupling increases in going from the La/Sr to La/Ca to Pr/Ca systems. This is consistent with the fact that the CE -type AFI state becomes stable in going from $\text{La}_{1/2}\text{Sr}_{1/2}\text{MnO}_3$

to $\text{La}_{1/2}\text{Ca}_{1/2}\text{MnO}_3$ to $\text{Pr}_{1/2}\text{Ca}_{1/2}\text{MnO}_3$. Therefore, it is reasonable to speculate that the orbital polarons still exist in metallic $\text{La}_{3/4}\text{Ca}_{1/4}\text{MnO}_3$ but cannot form a lattice to realize the FI phase because the electron-lattice coupling in $\text{La}_{3/4}\text{Ca}_{1/4}\text{MnO}_3$ is not strong enough compared to $\text{Pr}_{3/4}\text{Ca}_{1/4}\text{MnO}_3$. Actually, small ferromagnetic polarons are observed in $\text{La}_{1-x}\text{Ca}_x\text{MnO}_3$ ⁵ and their size is comparable to that of the orbital polaron shown in Fig. 1. The tendency to form orbital polarons discussed above may play a role in the phase separation.⁷ In particular, the important role of lattice distortion which follows from our results (see Fig. 3) may in principle help to explain the large scale phase separation observed in ref.⁸: In different degree of lattice distortion in different parts of the sample may stabilize respectively the homogeneous metallic phase in one of them and the CO insulating state in another, the charge densities in them being (almost) equal.

At the end of this section, let us discuss possible limitation of the present calculation. First, we cannot exclude the possibility that other lattice distortions would stabilize some charge and orbital orderings which are not considered here. For example, the Jahn-Teller distortion of LaMnO_3 -type would stabilize the charge and orbital ordering similar to that predicted for $x=1/8$ ¹⁵. With the hole-poor plane having the orbital ordering of LaMnO_3 , the hole-rich plane would have the hole concentration $x = 1/2$ and may have the CE -type state. However, it is not clear whether such layered structure would support a ferromagnetic state or not. Second, the Pr 4f orbitals are not included in the present model. It is possible that the Pr 4f-O $2p_\pi$ band accommodates some holes and, consequently, the effective hole concentration in the Mn 3d-O $2p_\sigma$ band is reduced. In order to check this possibility, one should study a model with the Pr 4f orbitals in future.

V. CONCLUSION

In conclusion, the model HF calculation indicates that orbital polarons, in which the orbitals of Mn^{3+} sites are directed towards the Mn^{4+} -like site and the spins are ferromagnetically aligned, are stabilized by the breathing-type and Jahn-Teller-type lattice distortions and that the magnetic coupling between these polarons is ferromagnetic. At $x = 1/4$, they form a body-centered cubic lattice (a form of charge ordering), which can be also viewed as a staggered arrangement of the orbital zigzags. Further theoretical and experimental studies are required in order to check whether the proposed structure is realized in $\text{Pr}_{3/4}\text{Ca}_{1/4}\text{MnO}_3$, and in general to clarify the importance of the orbital polarons and their relation to the CMR effect and to the phase separation.

ACKNOWLEDGEMENT

The authors are grateful to J. Hill, Y. Tomioka and Y. Tokura for informing us of their preliminary results on $\text{Pr}_{3/4}\text{Ca}_{1/4}\text{MnO}_3$ and for useful discussion. They would like to thank the kind hospitality of Lorentz Center, University of Leiden, where this work was initiated. This work was supported by the Netherlands Organization for Fundamental Research of Matter (FOM) and by the European network on Oxide Spin Electronics (OXSEN).

-
- ¹ J. B. Goodenough, Phys. Rev. **100**, 564 (1955); J. B. Goodenough and J. S. Zou, Nature **386**, 229 (1997).
 - ² A. Urushibara, Y. Moritomo, T. Arima, A. Asamitsu, G. Kido, and Y. Tokura, Phys. Rev. B **51**, 14103 (1995).
 - ³ K. Kubo and N. Ohata, J. Phys. Soc. Jpn. **33**, 21 (1972); N. Furukawa, J. Phys. Soc. Jpn. **64**, 2734 (1995).
 - ⁴ A. J. Millis, P. B. Littlewood, and B. I. Shalimov, Phys. Rev. Lett. **74**, 5144 (1995).
 - ⁵ J. M. De Teresa, M. R. Ibarra, P. A. Algarabel, C. Ritter, C. Marquina, J. Blasco, J. Garcia, A. del Moral, and Z. Arnold, Nature **386**, 256 (1997).
 - ⁶ A. Lanzara, N. L. Saini, M. Brunelli, F. Natali, A. Bianconi, P. G. Radaelli, and S.-W. Cheong, Phys. Rev. Lett. **81**, 878 (1998).
 - ⁷ A. Moreo, S. Yunoki, E. Dagotto, Science **283**, 2034 (1999); D. Arovas and F. A. Guinea, Phys. Rev. B **58**, 9150 (1998); M. Yu. Kagan, D. I. Khomskii and M. V. Mostovoy, Eur. Phys. J. B **12**, 217 (1999).
 - ⁸ M. Uehara, S. Mori, C. H. Chen, and S.-W. Cheong, Nature **399**, 560 (1999); M. Fäth, S. Freisem, A. A. Menovsky, Y. Tomioka, J. Aarts, and J. A. Mydosh, Science **285**, 1540 (1999).
 - ⁹ Z. Jirak, S. Krupicka, Z. Simsa, M. Dlouha, and S. Vratislav, J. Mag. Mag. Mat. **53**, 153 (1985).
 - ¹⁰ Y. Tomioka, A. Asamitsu, Y. Moritomo, H. Kuwahara, and Y. Tokura, Phys. Rev. Lett. **74**, 5108 (1995); H. Yoshizawa, H. Kawano, Y. Tomioka, and Y. Tokura, Phys. Rev. B **52**, R13145 (1995).
 - ¹¹ Y. Tokura and J. P. Hill, private communication.
 - ¹² Y. Yamada, O. Hino, S. Nohdo, R. Kanao, T. Inami, and S. Katano, Phys. Rev. Lett. **77**, 904 (1996).
 - ¹³ Y. Endoh, K. Hirota, S. Ishihara, S. Okamoto, Y. Murakami, A. Nishizaki, T. Fukuda, H. Kimura, H. Nojiri, K. Kaneko, and S. Maekawa, Phys. Rev. Lett. **82**, 4328 (1999).
 - ¹⁴ R. Kilian and G. Khaliullin, Phys. Rev. B **60**, 13458 (1999).
 - ¹⁵ T. Mizokawa, D. I. Khomskii, and G. A. Sawatzky, Phys. Rev. B **61**, R3776 (2000).
 - ¹⁶ A. E. Bocquet, T. Mizokawa, T. Saitoh, H. Namatame, and A. Fujimori, Phys. Rev. B **46**, 3771 (1992).
 - ¹⁷ W. A. Harrison, *Electronic Structure and the Properties of Solids*, (Dover, New York, 1989); P. Mahadevan, N. Shanathi, and D. D. Sarma, Phys. Rev. B **54**, 11199 (1996).

- ¹⁸ V. I. Anisimov, J. Zaanen, and O. K. Andersen, Phys. Rev. B **44**, 943 (1991).
- ¹⁹ T. Mizokawa and A. Fujimori, Phys. Rev. B **51**, 12880 (1995); Phys. Rev. B **54**, 5368 (1996).
- ²⁰ T. Mizokawa and A. Fujimori, Phys. Rev. B **56**, R493 (1997).
- ²¹ J. van den Brink, G. Khaliullin and D. I. Khomskii, Phys. Rev. Lett. **83**, 5118 (1999).

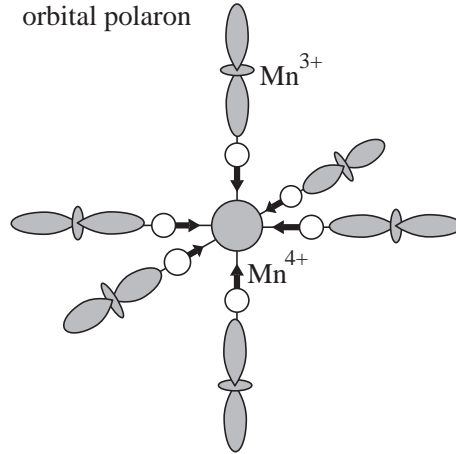


FIG. 1. Schematic drawings of the orbital polaron around Mn^{4+} -ion. The shaded orbitals and circles indicate the Mn^{3+} and Mn^{4+} sites, respectively. The open circles show the oxygen ions sitting between the Mn^{3+} and Mn^{4+} sites. The arrows indicate the shifts of the oxygen ions.

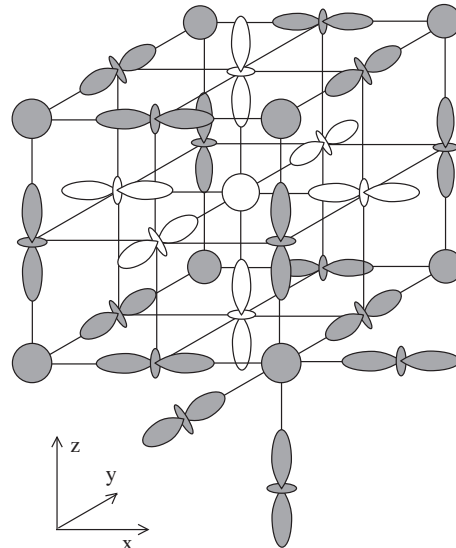


FIG. 2. Schematic drawing of the orbital polaron lattice for $\text{Pr}_{3/4}\text{Ca}_{1/4}\text{MnO}_3$. The shaded (open) orbitals and circles indicate Mn^{3+} and Mn^{4+} sites in sublattice A (B).

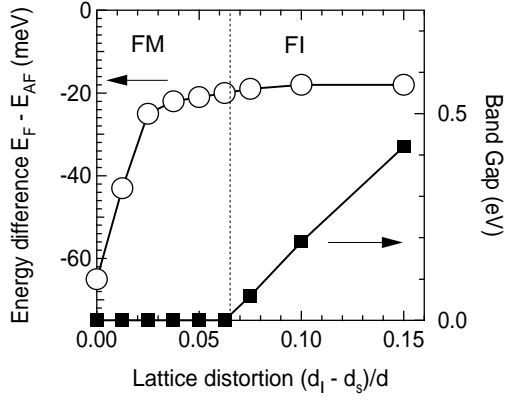


FIG. 3. Energy per formula unit cell of the ferromagnetic state (E_F) relative to the antiferromagnetic and insulating state (E_{AF}) as a function of the lattice distortion. The magnitude of the band gap for the ferromagnetic state is also plotted as a function of the lattice distortion. In the ferromagnetic (antiferromagnetic) state, spins in sublattice A are parallel (antiparallel) to those in sublattice B .

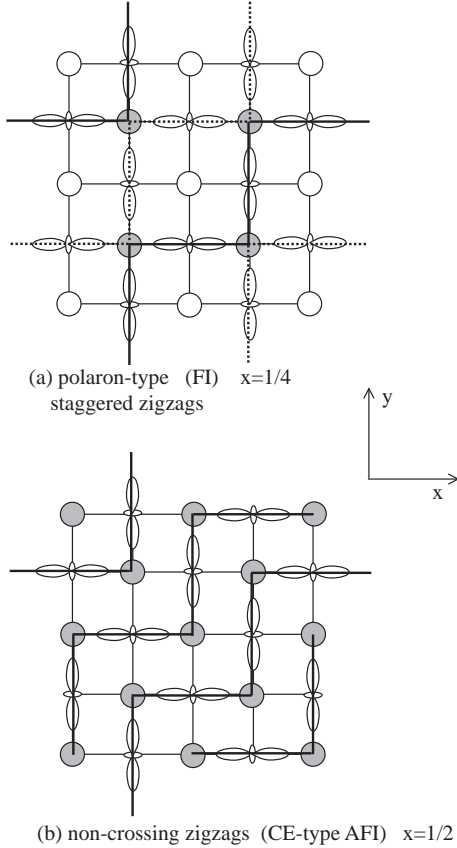


FIG. 4. Charge and orbital orderings in xy -plane (a) for $\text{Pr}_{3/4}\text{Ca}_{1/4}\text{MnO}_3$ and (b) for $\text{Pr}_{1/2}\text{Ca}_{1/2}\text{MnO}_3$. Shaded circles indicate Mn^{4+} sites and open circles indicate Mn^{3+} sites with the $3z^2 - r^2$ -type orbital. In $\text{Pr}_{3/4}\text{Ca}_{1/4}\text{MnO}_3$, the neighboring zigzags shown by solid and broken lines meet at the Mn^{4+} site. In $\text{Pr}_{1/2}\text{Ca}_{1/2}\text{MnO}_3$, the zigzags shown by the solid lines never meet each other.